Nonuniformity in Myocardial Accumulation of Fluorine-18-Fluorodeoxyglucose in Normal Fasted Humans

Robert J. Gropler, Barry A. Siegel, Kenneth J. Lee, Stephen M. Moerlein, David J. Perry, Steven R. Bergmann, and Edward M. Geltman

Division of Nuclear Medicine, Edward Mallinckrodt Institute of Radiology, St. Louis, Missouri and the Cardiovascular Division, Department of Internal Medicine, Washington University School of Medicine, St. Louis, Missouri

In initial studies using fluorine-18-fluorodeoxyglucose (FDG) in normal fasted subjects, we observed disparities in the regional myocardial accumulation of this tracer. Accordingly, we systematically evaluated regional myocardial FDG accumulation in comparison with regional myocardial perfusion assessed with oxygen-15-water and oxidative metabolism assessed with carbon-11-acetate in nine normal subjects (four studied after a 5-hr fast and five studied both fasted and following glucose loading). Under fasting conditions, myocardial accumulation of FDG in the septum and anterior wall averaged 80% of that in the lateral and posterior walls (p < 0.03). In contrast, after glucose loading the regional distribution of myocardial FDG accumulation became more homogeneous. Regional myocardial perfusion, oxidative metabolism, and accumulation of carbon-11-acetate were homogeneous under both conditions. Thus, under fasting conditions there are regional variations in myocardial accumulation of FDG, which are visually apparent, are not associated with concomitant changes in oxidative metabolism or perfusion, and cannot be attributed to partial-volume effects. This significant heterogeneity may limit the specificity of PET with FDG for detecting myocardial ischemia in fasting subjects.

J Nucl Med 1990; 31:1749–1756

Qualitative assessment of regional myocardial glucose utilization with fluorine-18- (^{18}F) fluorodeoxyglucose (FDG) and positron emission tomography (PET) is now being used clinically to evaluate patients with coronary artery disease (1–3). For example, in patients with ischemic cardiomyopathy, augmentation of glucose metabolism relative to flow has been shown to indicate a high likelihood of myocardial viability in zones of contractile dysfunction. Conversely, the pattern of concomitantly decreased glucose metabolism

and flow has been shown to represent myocardial necrosis or scar (1). Assessment of the pattern of regional glucose metabolism is now being incorporated into strategies designed to identify patients likely to benefit from myocardial revascularization (4).

FDG is a glucose analogue that traces the transmembranous transport and hexokinase-mediated phosphorylation of glucose. FDG-6-phosphate is then effectively trapped within the myocyte, because the sarcolemma is relatively impermeable to this intermediate, which is a poor substrate for further metabolism by either glycolytic or glycogen-synthetic pathways, and because dephosphorylation of FDG-6-phosphate is thought to be quite slow. The regional distribution of myocardial activity, assessed 40–60 min after i.v. administration of FDG (a time period that allows for adequate uptake and phosphorylation of the tracer), is thought to be related to overall (anaerobic and aerobic) regional glycolytic flux (5).

In normal myocardium, metabolism is primarily oxidative and utilizes various admixtures of substrates (free fatty acids, glucose, and lactate). The proportional contribution of each substrate to overall oxidative metabolism is dependent upon multiple factors, including arterial substrate content, the hormonal milieu, and the temporal relationship to a myocardial ischemic insult (6–8). For example, under fasting conditions, plasma insulin levels fall, resulting in lesser transport of glucose into the myocytes and an increase in the availability of free fatty acids secondary to increased lipolysis in peripheral adipose tissue. Under these conditions, free fatty acids become the preferred energy substrate for oxidative metabolism, while the contribution of glucose to total energy production via oxidative metabolism is decreased. Conversely, after feeding, plasma insulin levels rise, lipolysis within adipose tissue is inhibited, arterial fatty acid content decreases, and glucose becomes the primary substrate for oxidative metabolism (6). In ischemic myocardium, both the extraction of glucose and its rate of metabolism are increased in

myocytes by comparison with nonischemic tissue; under these circumstances, glucose also becomes the primary substrate for total energy production. The absolute myocardial accumulation of FDG is likely to be sensitive to the same factors that affect myocardial glucose utilization (9). Because of this dependence of myocardial uptake of FDG on these multiple factors, investigators using this tracer have attempted to standardize the metabolic environment by studying subjects either in the fasted state or following glucose loading, depending upon the metabolic question being addressed (10). For example, to detect the metabolic sequelae of ischemia in myocardium with normal resting contractile function, (e.g., after exercise induction of ischemia), the fasted state is preferred to accentuate the difference between ischemic tissue with increased accumulation of FDG and normal tissue with less uptake. Conversely, oral glucose loading is preferred to identify viable myocardium in zones of mechanical dysfunction, as ischemic tissue will accumulate FDG while necrotic tissue or scar will not take up this tracer (10).

Implicit in the interpretation of both quantitative PET data and images of the regional myocardial distribution of FDG, are the assumptions that the distribution of FDG is regionally homogeneous in normal myocardium and that the magnitude of any regional variability observed in diseased patients is greater than that observed in a normal population. Moreover, it is assumed that the regional distribution of activity in normal myocardium is independent of substrate availability.

In the course of performing baseline myocardial metabolic studies with FDG and carbon-11- (^{11}C) acetate, to assess myocardial oxidative metabolism in normal subjects under fasting conditions, we recently observed large regional disparities in the accumulation of FDG that were not present on the ^{11}C-acetate images. These initial observations suggested that the assumptions stated above may not be valid. Accordingly, we undertook this study to assess the regional variability of myocardial accumulation of FDG in normal individuals, under fasting conditions and after glucose loading. The regional distribution of FDG was compared to regional myocardial perfusion (measured with oxygen-15-water) and overall oxidative metabolism (measured with ^{11}C-acetate).

METHODS

Subjects

Nine healthy normal volunteers (five men, four women) with a mean age of 25.2 yr (range 22–29 yr) were studied. All were asymptomatic, had no history of cardiovascular disease, and had no significant risk factors for coronary artery disease, (i.e., hypertension, diabetes mellitus, hyperlipidemia, a history of cigarette smoking, or history of coronary artery disease in a first-degree relative). At the time of the study, eight of the subjects were not taking any medications and one subject was taking oral contraceptives. The experimental protocol was approved by the Human Studies Committee and the Radioactive Drug Research Committee of Washington University School of Medicine. Informed written consent was obtained from each subject.

Protocol

All subjects were studied after fasting for 5–8 hr. To examine the effects of substrate availability on regional myocardial FDG accumulation, five subjects (four men, one woman) underwent a repeat study after glucose loading. In these subjects, FDG was administered intravenously 2–3 hr after a high-carbohydrate meal and 1–2 hr after supplementation with 75 g glucose (Trutol®) orally.

The PET studies were performed with either Super PETT I or Super PETT IIB. Serial studies in any one subject were performed on the same tomograph. Super PETT I is a whole-body positron tomograph that permits the simultaneous acquisition of time-of-flight-corrected data sufficient for reconstruction of seven contiguous transaxial slices; the performance specifications of this device have been reported previously (11). Data were acquired in the high-resolution mode with an effective reconstructed slice separation of 11.4 mm and an in-plane reconstructed resolution of 13.5 mm (full width at half maximum). Super PETT IIB is a whole-body time-of-flight positron tomograph composed of four rings, each containing 320 barium fluoride crystals, permitting the acquisition of list-mode data sufficient to generate seven transaxial slices with a slice thickness of 9.0 mm and a center-to-center separation of 14 mm. The tomograph has a transverse field of view of 48 cm and an axial field of view of 11.2 cm; its intrinsic resolution in the transverse plane is better than 5.0 mm (full width at half maximum) and its axial resolution is 10.0 mm (full width at half maximum). With time-of-flight gain applied, the tomograph has a sensitivity of 158,000 cps/ μCi/cm^3. Data were reconstructed with a tomographic slice thickness of 11.0 mm and an in-plane reconstructed resolution of 12.2 mm (full width at half maximum). Activity detected with both tomographs was displayed in "PET" counts, which are linearly proportional to the true count rate.

At the beginning of the PET study, a transmission scan was obtained with a ^{68}Ge/^{68}Ga source external to the patient. This transmission scan was used to correct for attenuation of the emitted photons and to insure proper positioning of the subject. Stable positioning was assessed with the use of a low-energy laser and the placement of indelible marks on the subject's torso. A polyurethane mold of the torso and neck was constructed for each subject to minimize subject motion between data acquisitions and to facilitate repositioning for serial studies.

After completion of the transmission scan, the subject first underwent measurement of regional myocardial blood flow. This required acquisition of list-mode data for 150 sec commencing with the bolus i.v. injection of ^{15}O-water (0.25–0.30 mCi/kg body weight). Then, 40 mCi of ^{15}O-carbon monoxide were administered by inhalation to label the blood pool (see below), with the subsequent collection of list-mode data for 300 sec. Next, data to assess the regional myocardial accumulation of ^{11}C-acetate and to determine regional myocardial oxygen consumption were obtained in an 1800-sec list-mode collection that started immediately after the i. v. administration of ^{11}C-acetate (0.25–0.30 mCi/kg). Finally, data to assess

the distribution of myocardial FDG accumulation were obtained in an 1800-sec list-mode collection that was initiated 45 min after i.v. administration of 9–10 mCi of FDG.

Appropriate time delays to allow for decay of tracers were interspersed between each of these data collections. The time for completion of the entire PET study was ~2.5 hr. Heart rate and blood pressure were measured at regular intervals throughout the entire study. Venous blood samples were obtained for the determination of plasma concentrations of glucose, fatty acids, and acetate at the mid-point of the ^{11}C-acetate study and again 25–30 min after injection of FDG. Plasma glucose concentration was assayed with use of a commercially available enzymatic kit (Behring Diagnostics, La Jolla, CA) as was acetate (Boehringer Mannheim Biochemicals, Indianapolis, IN). Measurement of the concentration of free fatty acids was performed as described previously (12). Whenever possible, subjects remained in the tomograph for the entire study. In four cases for reasons of comfort, the subjects were removed from the tomograph after injection of FDG and were repositioned in the scanner just prior to the acquisition of the FDG data. Repositioning was performed as described above. The estimated radiation exposure (expressed as the effective dose equivalent) for two complete PET studies (fasting and after glucose loading) was 3.6 rems.

Analysis of PET Images

Depending upon the orientation of the heart within the thoracic cavity, two or three contiguous transaxial images, each containing interventricular septum were analyzed. Irregular regions of interest (ROIs) were defined interactively for the septum as well as the anterior, lateral, and posterior walls (Fig. 1). Activity (PET counts/pixel) in each region for each tomographic level were averaged to obtain an average value per region per subject. All ROIs were initially defined on the composite ^{11}C-acetate reconstructions (see below) and corresponding regions then were used on the FDG reconstructions. Identical regions were also used on the composite ^{15}O-water reconstructions (corrected for vascular activity as described below). Placement of irregular ROIs is quite reproducible with low interobserver and intraobserver variability (13).

Regional myocardial FDG activity was determined within the ROIs, defined as described above, on the composite FDG images reconstructed from the entire 30-min data collection. The regional activity measurements in PET counts/pixel were converted to percent of injected dose per cubic centimeter (% ID/cm^3) of myocardium, based on calibration of the tomographs with a uniform phantom, 20 cm in diameter, containing a known amount of positron-emitting radionuclide.

The ^{11}C-acetate data were reconstructed in two ways. First, reconstructions were generated representing ^{11}C-acetate data collected from 3–8 min after injection of the tracer. These images were employed for the placement of ROIs and for the assessment of the regional myocardial distribution of ^{11}C-acetate activity (expressed as % ID/cm^3). Data were also reconstructed in sequential 90-sec time intervals throughout the entire 30-min data collection. Time-activity curves were created for each ROI and analyzed with a multi-exponential least-squares curve-fitting algorithm as described previously (14). Data from the first 120–180 sec were excluded from this analysis, since they were influenced by continuing uptake of tracer and spillover of activity from the blood pool to the myocardium. In addition, because clearance of the tracer from

the blood is rapid (with only 10%–15% of peak activity remaining at 3 min), initiating the analysis of the time-activity curves at this time made correction for spillover of activity from the blood pool to the myocardium unnecessary (15). Although the algorithm is designed to fit each data set to a multi-exponential function, all curves confirmed best to a monoexponential fit. Previous studies have demonstrated that the myocardial turnover rate constant, k$_1$, describing the clearance of ^{11}C activity from the myocardium (after the injection of ^{11}C-acetate) correlates closely with myocardial oxygen consumption (15–17). This rate constant and the corresponding biologic half-time (t$_{\frac{1}{2}}$), calculated as (ln 2)/k$_1$, were determined for each ROI.

Data acquired after the administration of ^{15}O-water were reconstructed in two ways. For the visualization of the heart, a composite reconstruction was created from data acquired for 120 sec after the arrival of the bolus in the left atrium. Images of relative perfusion were generated by correcting the 120-sec composite ^{15}O-water reconstruction for activity emanating from the intravascular compartment with use of the 300-sec composite ^{15}O-carbon monoxide image, as previously described (13). These images were used only for the placement of ROIs for subsequent quantitative analysis of the dynamic data. For the quantitative analysis, 18 sequential 5-sec reconstructions were generated for each tomographic level beginning with the arrival of the bolus in the left atrium. For determination of the arterial input curve necessary for quantification, an additional ROI (1.25 cm^3) was defined in the left atrial cavity (on the most basal transaxial ^{15}O-carbon monoxide image that contained left atrium). Data were obtained for each ROI in each of the 5-sec ^{15}O-water reconstructions at each tomographic level. Myocardial blood flow in absolute terms was then calculated with a technique incorporating a modified one-compartment model developed and validated previously in our laboratory (18, 19).

Preparation of Tracers

Oxygen-15 water, ^{15}O-carbon monoxide, ^{11}C-acetate, and FDG were prepared as previously described (16,20–22). Radiochemical purities of ^{11}C-acetate and FDG were typically >99%.

Statistical Methods

The results for continuous variables are presented as mean values and standard deviations. Comparisons of independent or paired samples were subjected to analysis of variance followed by t-tests corrected for the number of comparisons by the Bonferroni method. Due to the fairly wide variability in substrate levels between individuals, the significance of differences between groups for serum substrate levels were determined with a Mann-Whitney rank-sum method. Probability (p) values of <0.05 were considered statistically significant.

RESULTS

Assessment of Regional Myocardial FDG Accumulation

In two subjects studied after 5-8 hr of fasting, myocardial FDG images were uninterpretable because of minimal myocardial accumulation of tracer, presumably reflecting preferential fatty acid utilization and decreased utilization of glucose by the myocardium. These two subjects (who were not studied in the fed

TABLE 1
Distribution of Myocardial Activity Under Fasting Conditions and Following Glucose Loading

	Fasting (n = 7)		Post-Glucose (n = 5)	
	FDG	^{11}C-acetate	FDG	^{11}C-acetate
Septum	0.65 ± 0.45*	0.98 ± 0.40	0.88 ± 0.29	1.10 ± 0.16
Anterior wall	0.68 ± 0.44*	0.94 ± 0.35	0.90 ± 0.31	0.96 ± 0.19
Lateral wall	0.87 ± 0.51	1.02 ± 0.38	1.00 ± 0.27	1.01 ± 0.15
Posterior wall	0.80 ± 0.51	1.01 ± 0.43	1.07 ± 0.32	1.08 ± 0.16

Results expressed as mean ± s.d. % ID/cm$^3 \times$ 10^{-2}.
* p < 0.03 compared with lateral and posterior walls under fasting conditions.

state) were excluded from further analyses. In the remaining seven subjects, the PET images were of adequate quality to permit evaluation of the regional myocardial distribution of FDG. Significant regional disparities in the myocardial accumulation of FDG were noted in these subjects (Table 1). Mean activity in the septum and anterior wall averaged 80% of that in the lateral and posterior walls (p <0.03). This decreased activity resulted in a visually apparent defect on the tomographic images obtained 45 min after injection (Fig 2). Activity in the posterior wall was not significantly different from that in the lateral wall.

In contrast to the marked differences in regional myocardial FDG accumulation observed under fasting conditions, myocardial FDG activity was more homogeneously distributed after glucose loading in the five subjects so studied. No statistically significant differences in regional activities were observed (Table 1), and defects were less apparent on visual inspection of the images (Fig 2). Although the data suggest overall greater myocardial FDG uptake after glucose loading, the fasting and fed uptake values were not significantly different.

Myocardial Accumulation and Clearance of ^{11}C-Acetate

The regional distribution of myocardial ^{11}C activity was assessed using the composite reconstructions of data acquired 3–8 min after injection of ^{11}C-acetate.
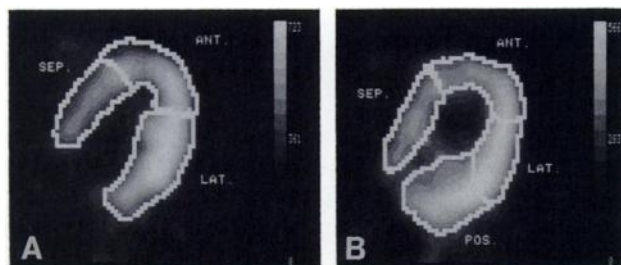

FIGURE 1
Two transverse tomographic reconstructions of left ventricular myocardium demonstrating the placement of irregular ROIs. The image on the left is at the (A) mid-ventricular level while the image on the right is (B) at a more apical level.

This interval was chosen because previous studies in normal subjects have shown this to be the period of peak myocardial accumulation of ^{11}C-acetate. In fasting subjects, the regional myocardial distribution of ^{11}C activity was homogeneous, unlike that of FDG (Table 1 and Fig. 2). Following glucose loading, the regional distribution of activity did not change significantly (Table 1).

The clearance of regional ^{11}C activity from the myocardium, which reflects oxidative metabolism, was measured to determine whether the regional differences in myocardial accumulation of FDG observed under fasting conditions were paralleled by differences in regional myocardial oxidative metabolism. In all cases, myocardial clearance of ^{11}C activity was monoexponential. After fasting, regional oxidative metabolism was homogeneous with average regional k_1 values ranging from 0.044 ± 0.008 min^{-1} to 0.051 ± 0.005 min^{-1}, with the corresponding $t_{1/2}$ values ranging from 13.5 ± 1.3 min to 15.7 ± 2.7 min (Table 2). After glucose loading, the regional clearance continued to be homogeneous with average regional values for k_1 ranging from 0.045 ± 0.011 min^{-1} to 0.058 ± 0.019 min^{-1}, with the corresponding $t_{1/2}$ values ranging 12.0 ± 3.9 min to 15.5 ± 3.8 min (Table 2). There was a slight, but statistically insignificant increase in the rate of ^{11}C activity clearance from the myocardium with glucose loading. It has been demonstrated previously that the clearance of ^{11}C activity from the myocardium is insensitive to alterations in substrate availability (17), and thus the slight increase we observed was probably secondary to the mild increase in the rate-pressure product that occurred after glucose loading (see below).

Regional Myocardial Perfusion

To determine whether regional variability in substrate utilization was due to altered substrate delivery, regional myocardial perfusion was measured by PET with ^{15}O-water. Regional perfusion was homogeneous both under fasting conditions and after glucose loading (Table 2). In addition, perfusion in absolute terms did not change significantly with altered substrate availability (Table 2).
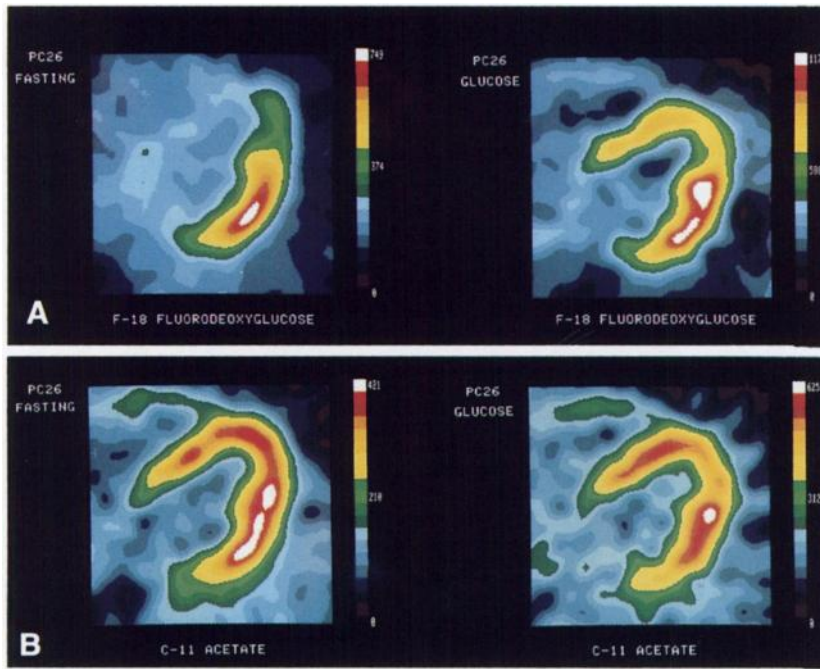
FIGURE 2
Four transverse midventricular tomographic reconstructions from data acquired 45–75 min after i.v. infusion of [^{18}F]FDG and 3–8 min after i.v. infusion of ^{11}C-acetate, in the same subject, under fasting conditions and following glucose loading. (A) Regional myocardial accumulation of FDG and (B) regional myocardial accumulation of ^{11}C-acetate. The top of each image represents anterior, and the left of each image represents the patient's right. Under fasting conditions, large regional disparities of myocardial accumulation of FDG are present with the regional distribution of activity becoming more homogeneous after glucose loading. Conversely, the distribution of ^{11}C-acetate myocardial activity is homogeneous both under fasting conditions and following glucose loading.

Hemodynamic Changes

Hemodynamic measurements recorded during the collection of ^{11}C-acetate and FDG data are presented in Table 3. The rate-pressure product (RPP) [heart rate x systolic blood pressure], an index of global myocardial work, was calculated for all subjects. Under fasting conditions, heart rate, systolic blood pressure, and RPP did not vary significantly between the ^{11}C-acetate and FDG collections. After glucose loading, the heart rate, systolic blood pressure, and RPP all increased slightly, but not significantly, when compared with the fasting measurements. These increases probably reflect a slight, but transient increase in serum osmolality that occurs following glucose loading. However, after glucose loading, the systolic blood pressure and RPP were signifi-

cantly higher during the FDG collection than during the ^{11}C-acetate collection. The explanation for these differences is unclear.

Analysis of Plasma Concentrations of Metabolites

Plasma concentrations of glucose, nonesterfied fatty acids, and acetate measured during the ^{11}C-acetate and FDG collections are presented in Table 3. Fasting glucose concentrations were within the normal range for healthy nondiabetic humans and had returned to the normal range by 1.5–2.0 hr after glucose loading. The plasma concentrations for nonesterified fatty acids were also within the normal range for fasting humans. After glucose loading, the concentrations of nonesterified fatty acids decreased significantly (p < 0.05). Acetate

TABLE 2
Regional Myocardial Blood Flow and Kinetics of Regional Myocardial ^{11}C Activity Under Fasting Conditions and Following Glucose Loading

	Region	Flow (ml/g/min)	k_1 (min^{-1})	$t_{1/2}$ (min)
Fasting (n = 7)	Septum	1.17 ± 0.44	0.051 ± 0.005	13.5 ± 1.3
	Anterior wall	1.36 ± 0.36	0.048 ± 0.008	14.2 ± 2.5
	Posterior wall	1.07 ± 0.36	0.045 ± 0.012	15.2 ± 3.9
	Lateral wall	1.24 ± 0.22	0.044 ± 0.008	15.7 ± 2.9
Post-Glucose (n = 5)	Septum	0.98 ± 0.36	0.058 ± 0.019	12.0 ± 3.9
	Anterior wall	0.97 ± 0.29	0.052 ± 0.006	13.2 ± 1.4
	Posterior wall	0.80 ± 0.17	0.045 ± 0.011	15.5 ± 3.8
	Lateral wall	0.84 ± 0.29	0.049 ± 0.006	13.9 ± 1.8

Values represent mean ± s.d.
F statistic not significant under fasting conditions and following glucose loading.
No significant differences comparing regional values under fasting conditions with those following glucose loading.

TABLE 3
Hemodynamics and Venous Substrate Concentrations Under Fasting Conditions and Following Glucose Loading

	HR (min⁻¹)	SBP (mmHg)	RPP (mm Hg/min)	Glucose (mmol/liter)	NEFA (μmole/ liter)	Acetate (μmole/liter)
Fasting (n = 7)						
Acetate scan	69 ± 8	117 ± 14	8077 ± 1744	5.1 ± 0.7	527 ± 84	423 ± 393
FDG scan	68 ± 9	118 ± 14	8044 ± 1613	5.2 ± 0.7	530 ± 102	252 ± 206
mean	68 ± 8	118 ± 14	8061 ± 1598	5.1 ± 0.7	529 ± 93	338 ± 299
Post-Glucose (n = 5)						
Acetate scan	70 ± 7	123 ± 12	8880 ± 1776	5.3 ± 1.1	262 ± 124	162 ± 195
FDG scan	74 ± 3	129 ± 20*	9453 ± 1770*	4.6 ± 0.9	270 ± 129	106 ± 79
mean	72 ± 5	127 ± 20	9167 ± 1767	5.2 ± 0.6	266 ± 126†	134 ± 137

Values represent mean ± s.d.
HR = heart rate; SBP = systolic blood pressure; RPP = rate-pressure product; and NEFA = nonesterfied fatty acid.
* $p < 0.05$ compared with RPP measured during ¹¹C-acetate collection following glucose loading.
† $p < 0.05$ compared with fasting values.

levels were highly variable, both during fasting and after glucose loading, but appeared to decrease slightly ($p = ns$) in response to the latter intervention.

DISCUSSION

We have demonstrated that there is significant non-uniformity in the regional distribution of FDG within normal human myocardium in the fasted state. Moreover, we have shown that the regional myocardial distribution of FDG is dependent on plasma substrate levels, with such regional disparities becoming less prominent after administration of glucose and concomitant lowering of plasma fatty acid concentrations. Our results demonstrate systematically that previous anecdotal reports of regional differences in accumulation of FDG by normal myocardium (2,23) have identified a biologically significant phenomenon of considerable magnitude with respect to interpretation of tomographic images.

The sensitivity of global myocardial accumulation of FDG to arterial substrate concentrations is well established (9). Under fasting conditions, the combination of decreased plasma insulin levels and increased plasma concentrations of free fatty acids results in a reduction in myocardial glucose utilization and, thus, in FDG accumulation by the heart. Conversely, after glucose loading, the increase in plasma insulin levels coupled with the decreased serum concentration of free fatty acids results in an increase in myocardial glucose utilization, which is reflected by an increase in the accumulation of FDG by the heart (9). The magnitude of the change in uptake in response to changing plasma concentration of substrate may vary, but since the entire myocardium is exposed to the same concentration of substrate, the distribution of uptake should be uniform. In concordance with previous reports (24) and despite

the controlled duration of fasting in this study, the myocardial accumulation of FDG in the fasted state was quite variable; two of nine subjects had minimal myocardial uptake of FDG, rendering the images uninterpretable for delineation of myocardium. However, in the remaining seven subjects, in whom myocardial FDG uptake was visible on the images, significant heterogeneity in the regional distribution of this tracer was noted. The septum and anterior wall had significantly less activity than the lateral and posterior walls. After glucose loading, the distribution of FDG within myocardium became nearly homogeneous, although, the pattern of decreased FDG uptake in the septal and anterior walls compared with that in the lateral and posterior walls was still evident. As expected, there was a trend towards greater myocardial accumulation of FDG after glucose loading than in the fasted state.

Decreased count recovery secondary to partial-volume effects is a well recognized limitation of cardiac PET imaging (25). In transaxial tomographic reconstructions at the mid-ventricular level, the septal and anterior walls appear thinner than the lateral and posterior walls, and the apparent disparity in activity of these walls is compounded by the posterior papillary muscle, which is contiguous with the lateral and posterior walls. As a consequence, observed counts will be less in the septal and anterior walls when compared with the lateral and posterior walls. It is this effect that has been postulated as the explanation for the earlier anecdotal observations of heterogeneous myocardial accumulation of FDG in normal subjects (2,23). Under fasting conditions the regional myocardial distribution of ¹¹C activity was homogeneous on the same tomographic slices exhibiting significant disparities in FDG accumulation. Since the effects of partial-volume sampling would equally affect all reconstructions in the same subject at the same tomographic level, decreased

count recovery in the septum and anterior wall due to partial-volume effects is an unlikely explanation for the heterogenous regional distribution of myocardial FDG activity in the fasted state.

Regional differences in myocardial contractile work could potentially account for the regional disparities in myocardial accumulation of FDG. Although we did not directly assess regional left ventricular function, it is unlikely for several reasons that there were regional differences in myocardial contractile work in our subjects. First, all of the subjects were under 30 yr of age and healthy and, thus, have a very low likelihood of regional left ventricular contractile dysfunction due to cardiac disease. Second, because the regional differences in myocardial accumulation of FDG were sensitive to the availability of substrate it would have to be postulated that regional mechanical function is sensitive to levels of serum substrates as well. No data in the literature support this hypothesis. Third, although some studies have demonstrated increased excursion and more rapid thickening of the posterior and lateral walls when compared with the septum and anterior walls in normal humans (26,27), the results from these studies are quite variable and may simply be a function of the imaging modality or the reference system. Finally, myocardial contractile function is a major determinant of myocardial oxygen consumption (28) and the turnover rate constant for ^{11}C activity in myocardium after the administration of ^{11}C-acetate correlates closely with myocardial oxygen consumption over a wide range of levels of cardiac work (14–17). Thus, if regional differences in myocardial work were present in our subjects there should be parallel disparities in the clearance of ^{11}C activity from the tissue. Instead, we found nearly homogeneous clearance of ^{11}C activity from the myocardium, which is in agreement with the results of previous studies from our laboratory (29).

Regional variations in myocardial perfusion with resultant parallel disparities in delivery of tracer potentially could account for the heterogeneous distribution of regional FDG activities observed under fasting conditions. Regional perfusion was measured in absolute terms with ^{15}O-water. Regional perfusion was homogeneous both under fasting conditions and after glucose loading. Our finding of homogeneous regional perfusion in normal human myocardium, is consistent with previous studies from our laboratory and from others using different flow tracers (18,30,31), and makes it unlikely that regional differences in tracer delivery account for the heterogeneity in FDG activity.

Under homeostatic conditions, where the rate of glycogen synthesis should equal the rate of glycogen breakdown, regional myocardial FDG activity has been demonstrated to reflect regional myocardial glycolytic flux (5). Consequently, our data suggest that, in normal myocardium glucose flux in the septum and anterior wall is lower than that in the lateral and posterior walls with the magnitude of the regional differences being greater under fasting conditions than that after glucose loading. The overall rate of oxidative metabolism is similar in all four walls. A potential explanation for these observations is that differences in regional rates of glucose metabolism, in absolute terms, are constant and independent of substrate availability. Thus, relative regional differences in glucose flux would be more pronounced when overall myocardial glucose utilization is low (such as under fasting conditions) than when myocardial glucose utilization is high (such as after glucose loading). Although a myocardial gradient for glycogen, total phosphorylase activity, and phosphorylase "a" activity exists from endocardium to epicardium in experimental animals (32), no such gradient has been reported in humans. Preliminary experimental studies with dogs showed no regional disparities in FDG accumulation assessed by direct well spectroscopy (Bergmann SR, et al., unpublished observations). Moreover, the existence of such a gradient would not explain why, the septum and anterior wall have different rates of net glucose flux than the lateral and posterior walls.

Clinical Implications

Normal human myocardium manifests significant regional disparities in the accumulation of FDG under fasting conditions, with the septum and anterior wall containing significantly less activity than the lateral and posterior walls. Moreover, the regional distribution of FDG activity is extremely sensitive to substrate availability. Nevertheless, assessment of regional myocardial glucose utilization is now being used in the clinical setting to evaluate patients with coronary artery disease (1,3). Depending upon the metabolic question that is being addressed, patients are generally studied in the fasted state (to detect myocardial ischemia) or after glucose loading (to identify viable but mechanically dysfunctional myocardium) (10). Our finding of significant heterogeneity in regional accumulation of FDG by normal myocardium under fasting conditions suggests that the specificity of FDG imaging may be limited for the detection of myocardial ischemia or in any other situation where the study is performed in the fasted state. It therefore appears essential to recognize that results of cardiac PET studies with FDG are likely to be definitive under those conditions in which the metabolic question of interest can be optimally answered with the patient studied in the postprandial state.

ACKNOWLEDGMENTS

REFERENCES

1. Tillisch J, Brunken R, Marshall R, et al. Reversibility of cardiac wall-motion abnormalities predicted by positron tomography. *N Engl J Med* 1986; 314:884–888.
2. Camici P, Araujo LI, Spinks T, et al. Increased uptake of ^{18}F-fluorodeoxyglucose in postischemic myocardium of patients with exercise-induced angina. *Circulation* 1986; 74:81–88.
3. Fudo T, Kambara H, Hashimoto T, et al. F-18-deoxyglucose and stress N-13-ammonia positron emission tomography in anterior wall healed myocardial infarction. *Am J Cardiol* 1988; 61:1191–1197.
4. Brunken RC, Shelbert HR. Positron emission tomography in clinical cardiology. *Cardiol Clin* 1989; 7:607–629.
5. Ratib O, Phelps ME, Huang SC, Henze E, Selin CE, Shelbert HR. Positron tomography with deoxyglucose for estimating local myocardial glucose metabolism. *J Nucl Med* 1982; 23:577–586.
6. Camici P, Ferrannini E, Opie LH. Myocardial metabolism in ischemic heart disease: basic principles and application to imaging by positron emission tomography. *Prog Cardiovasc Dis* 1989; 32:217–238.
7. Merhige ME, Ekas RD, Mossberg K, Taegtmeyer HT, Gould KL. Catecholamine stimulation, substrate competition, and myocardial glucose uptake in conscious dogs assessed with positron emission tomography. *Circ Res* 1987; 61:124–129.
8. Myears DW, Sobel BE, Bergmann SR. Substrate use in ischemic and reperfused canine myocardium: quantitative considerations. *Am J Physiol* 1987; 253:H107–H114.
9. Phelps ME, Hoffman EJ, Selin SC, et al. Investigation of [18F] 2-fluoro-2-deoxyglucose for the measure of myocardial glucose metabolism. *J Nucl Med* 1978; 19:1311–1319.
10. Gould KL. Myocardial metabolism by positron emission tomography in hypertrophic cardiomyopathy. *J Am Coll Cardiol* 1989; 13:325–326.
11. Ter-Pogossian MM, Ficke DC, Yamamoto M, Hood JT. Super PETT I: a positron emission tomograph utilizing photon time-of-flight information. *IEEE Trans Med Imag* 1982; 3:179–187.
12. Bergmann SR, Carlson E, Dannen E, Sobel BE. An improved assay with 4-(2-thiazlylaso)-resorcinol for non-esterified fatty acids in biological fluids. *Clin Chim Acta* 1980; 104:53–63.
13. Walsh MN, Bergmann SR, Steele RL, et al. Delineation of impaired regional myocardial perfusion by positron emission tomography with H2[15]O. *Circulation* 1988; 78:612–620.
14. Henes CG, Bergmann SR, Walsh MN, Sobel BE, Geltman EM. Assessment of myocardial oxidative metabolic reserve with positron emission tomography and carbon-11-acetate. *J Nucl Med* 1989; 30:1489–1499.
15. Brown MA, Myears DW, Bergmann SR. Noninvasive assessment of canine myocardial oxidative metabolism with carbon-11-acetate and positron emission tomography. *J Am Coll Cardiol* 1988; 12:1054–1063.
16. Brown MA, Marshall DR, Sobel BE, Bergmann SR. Deline-

ation of myocardial oxygen utilization with carbon-11-acetate. *Circulation* 1987; 76:687–696.
17. Brown MA, Myears DW, Bergmann SR. Validity of estimates of myocardial oxidative metabolism with carbon-11-acetate and positron emission tomography despite altered patterns of substrate utilization. *J Nucl Med* 1989; 30:187–193.
18. Bergmann SR, Herrero P, Markham J, Weinheimer CJ, Walsh MN. Noninvasive quantitation of myocardial blood flow in human subjects with oxygen-15-labeled water and positron emission tomography. *J Am Coll Cardiol* 1989; 14:639–652.
19. Herrero P, Markham J, Bergmann Sr. Quantitation of myocardial blood flow with H2[15]O and positron emission tomography: assessment and error analysis of a mathematical approach. *J Comput Assist Tomgr* 1989; 13:862–873.
20. Welch MJ, Kilbourn MR. A remote system for the routine production of oxygen-15 radiopharmaceuticals. *J Lab Comp Radiopharm* 1985; 22:1193–1200.
21. Welch MJ, Ter-Pogossian MM. Preparation of short half-lived radioactive gases for medical studies. *Radiat Res* 1968; 36:580–587.
22. Moerlein SM, Brodack JW, Siegel BA, Welch MJ. Elimination of contaminant kryptofix 2.2.2 in the routine production of 2-[18F]fluoro-2-deoxy-D-glucose. *Int J Rad Appl Instrum [A]* 1989; 40:741–743.
23. Marshall RC, Tillisch JH, Phelps ME, et al. Identification and differentiation of resting myocardial ischemia and infarction in man with positron computed tomography, ^{18}F-labeled fluorodeoxyglucose and N-13-ammonia. *Circulation* 1982; 67:766–778.
24. Grover-McKay M, Schwaiger M, Krivokapich JK, Perloff K, Phelps ME, Shelbert HR. Regional myocardial blood flow and metabolism at rest in mildly symptomatic patients with hypertrophic cardiomyopathy. *J Am Coll Cardiol* 1989; 13:317–324.
25. Hoffman EJ, Huang SC, Phelps ME. Quantitation in positron emission computed tomography. 1. Effect of object size. *J Comput Assist Tomgr* 1979; 3:299–308.
26. Kong Y, Morris JJ Jr, McIntosh HD. Assessment of regional myocardial performance from biplane cineangiograms. *Am J Cardiol* 1971; 27:529–537.
27. Shapiro E, Marier DL, St. John-Sutton MG, et al. Regional non-uniformity of wall dynamics in the normal left ventricle. *Br Heart J* 1981; 45:264–270.
28. Braunwald E, Sobel BE. Coronary blood flow and myocardial ischemia. In: Braunwald E, ed. *Heart disease. A textbook of cardiovascular medicine*, 3rd edition. Philadelphia: W.B. Saunders; 1988:1191–1221.
29. Walsh MN, Geltman EM, Brown MA, et al. Noninvasive estimation of regional myocardial oxygen consumption by positron emission tomography with carbon-11-acetate in patients with myocardial infarction. *J Nucl Med* 1989; 30:1798–1808.
30. Iida H, Kanno I, Takahashi A, et al. Measurement of absolute myocardial blood flow with H2[15]O and dynamic positron emission tomography. Strategy for quantitation in relation to partial-volume effect. *Circulation* 1988; 78:104–115.
31. Krivokapich J, Smith GT, Huang SC, et al. ^{13}N-ammonia myocardial imaging at rest and with exercise in normal volunteers. Quantification of absolute myocardial perfusion with dynamic positron emission tomography. *Circulation* 1989; 80:1328–1337.
32. Jedeikin LA. Regional distribution of glycogen and phosphorylase in the ventricles of the heart. *Circ Res* 1964; 14:202–211.